Thioether Binding of Manganese Oxidation States. Chemistry of an $Mn^{II,III}S_2N_2O_2$ Family

Partha Chakraborty, Swapan Kumar Chandra, and Animesh Chakravorty*

Department of Inorganic Chemistry, Indian Association for the Cultivation of Science,
Calcutta 700 032, India

Received June 16, 1993[®]

Reaction of manganese(II) acetate tetrahydrate with dithiaalkyl-substituted triazene 1-oxides, $[RN(O)NNHC_6H_4S]_2(CH_2)_x$ (H_2RxL; R = Me, Ph; x = 2, 3), have afforded $Mn^{II}(RxL)$, from which $[Mn^{III}(RxL)]Y$ ($Y^- = ClO_4^-, PF_6^-$) have been electrochemically synthesized. The X-ray structures of three complexes are reported: (i) Mn(Me2L), chemical formula $C_{16}H_{18}N_6O_2S_2Mn$, crystal system monoclinic; space group $P2_1/a$, a = 19.465(6) Å, b = 7.933(4) Å, c = 26.644(7) Å, β = 110.19(2)°, V = 3861(2) Å^3, Z = 8, R = 6.27%, R_w = 6.59%; (ii) Mn(Me3L), chemical formula $C_{17}H_{20}N_6O_2S_2Mn$, crystal system monoclinic, space group $P2_1/n$, a = 7.774(3) Å, b = 10.033(5) Å, c = 25.583(14) Å, β = 92.19(4)°, V = 1994(1) Å^3, Z = 4, R = 5.40%, R_w = 5.50%; (iii) $[Mn(Me2L)]PF_6\cdot CH_2Cl_2$, chemical formula $C_{17}H_{20}N_6O_2S_2Cl_2PF_6Mn$, crystal system monoclinic, space group $P2_1/n$, a = 12.361(3) Å, b = 14.621(3) Å, c = 14.941(3), Å, β = 101.24(2)°, V = 2649(1) Å^3, Z = 4, R = 7.68%; R_w = 6.70%. In each case, the ligand acts in a hexadentate fashion, affording distorted octahedral $MnS_2N_2O_2$ coordination spheres. The Mn–S(thioether) distances in Mn(Me2L) and Mn(Me3L), 2.677(3)–2.783(4) Å, are significantly longer than those in $[Mn(Me2L)]PF_6\cdot CH_2Cl_2$, 2.500(4) and 2.502(4) Å. All the complexes are high-spin, and the manganese(II) species are EPR-active. The Mn(MexL)–Mn(MexL)$^+$ redox pair forms a quasireversible cyclic voltammetric couple, the $E_{1/2}$ values in acetonitrile lying in the range 0.37–0.48 V vs SCE.

Introduction

As a member of the sulfide–thiolate–thioether triad and as an isoelectronic neighbor of the tertiary phosphine function, the thioether group is of inherent interest as a ligand.[1-3] It is, however, a weak σ-donor-cum-π-acceptor and it is also unable to neutralize cationic charge. As a result, thioethers remained a lesser partner in the burgeoning transition metal chemistry of sulfur ligands. Noteworthy progress in thioether coordination chemistry has taken place in recent years through utilization of multidentate ligands, especially macrocycles.[2,3]

Some areas however continue to remain in a state of poor development. Of special interest to us is the case of manganese, for which authentic thioether ligated species are very rare.[1-6] As part of our program on manganese oxidation states,[7] we have undertaken a planned search for new thioether-ligated species, and herein we describe the synthesis and characterization of a family of complexes of coordination type $MnS_2N_2O_2$. The accessible and electrochemically interconvertible metal oxidation states are +2 and +3, both of which have been isolated in the crystalline state. The X-ray structures of one manganese(III) and two manganese(II) complexes are reported, providing the first measure of the Mn^{II}–S(thioether) bond and a unique opportunity for comparing it with that of the corresponding Mn^{III}–S bond.

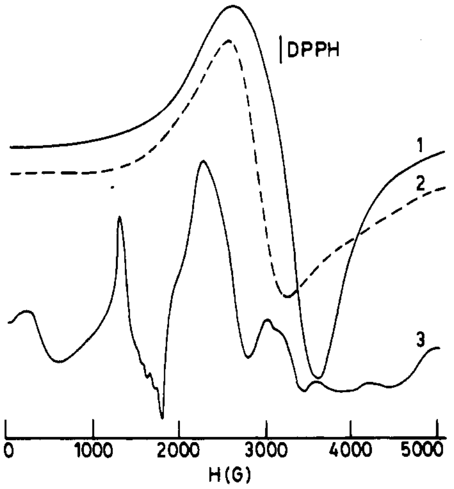

Figure 1. EPR spectra at X-band of Mn(Me2L): in dichloromethane–toluene (1:1) at 300 K (—, 1); in the polycrystalline state at 300 K (- - -, 2); in dichloromethane–toluene (1:1) at 77 K (—, 3). Instrument settings: power, 30 dB; modulation, 100 kHz; sweep center, 3200 G; sweep width, 8000 G; sweep time, 240 s.

Results and Discussion

Synthesis and Characterization. In this work multiple chelation by acyclic polydentate ligands bearing anionic charges has been utilized as the stabilizing principle.[8] Our familarity with hexadentate triazene 1-oxide substituted thioether ligands[9,10] has prompted us test them for binding manganese oxidation states. The three ligands used in the present work are of type **1**,

---

[®] Abstract published in *Advance ACS Abstracts,* October 1, 1993.

(1) Murray, S. G.; Hartley, F. R. *Chem. Rev.* **1981,** *81,* 365.

(2) Blake, A. J.; Schröder, M. *Adv. Inorg. Chem.* **1990,** *35,* 1.

(3) Cooper, S. R.; Rawle, S. C. *Struct. Bonding (Berlin)* **1990,** *72,* 1.

(4) Doedens, R. J.; Veal, J. T.; Little, R. G. *Inorg. Chem.* **1975,** *14,* 1138.

(5) Elias, H.; Schmidt, C.; Küppers, H.-J.; Wieghardt, K.; Nuber, B.; Weiss, J. *Inorg. Chem.* **1989,** *28,* 3021.

(6) Tomita, M.; Matsumota, N.; Agaki, H.; Ōkawa, H.; Kida, S. *J. Chem. Soc., Dalton Trans.* **1989,** 179.

(7) (a) Manivannan, V.; Dutta, S.; Basu, P.; Chakravorty, A. *Inorg. Chem.* **1993,** *32,* 769. (b) Chandra, S. K.; Chakraborty, P.; Chakravorty, A. *J. Chem. Soc., Dalton Trans.* **1993,** 863. (c) Chandra, S. K.; Chakravorty, A. *Inorg. Chem.* **1992,** *31,* 760 and references therein.

(8) (a) Choudhury, S. B.; Ray, D.; Chakravorty, A. *Inorg. Chem.* **1991,** *30,* 4354. (b) Choudhury, S. B.; Ray, D.; Chakravorty, A. *J. Chem. Soc., Dalton Trans.* **1992,** 107.

(9) Ray, D.; Pal, S.; Chakravorty, A. *Inorg. Chem.* **1986,** *25,* 2674.

(10) Karmakar, S.; Choudhury, S. B.; Ray, D.; Chakravorty, A. *Polyhedron* **1993,** *12,* 291.

0020-1669/93/1332-5349$04.00/0

Table I. Magnetic Moments, EPR *g* Factors, and Electronic Spectral Data

compd	μ_{eff},[a] μ_B	*g*	UV–vis data:[b] λ_{max}, nm (ϵ, $M^{-1}\,cm^{-1}$)
Mn(Me2L)	5.86	2.009;[c] 2.228;[d] 2.242[e]	480[f] (130), 340 (9600)
Mn(Ph2L)	5.87	2.168,[d] 4.862;[d] 2.182,[e] 4.829[e]	550[f] (140), 340 (14 300)
Mn(Me3L)	5.88	2.547,[d] 5.135;[d] 2.463,[e] 4.964[e]	540[f] (140), 340 (16 900)
[Mn(Me2L)]$PF_6 \cdot CH_2Cl_2$	4.86		1000 (400), 580[f] (300), 400 (4100)
[Mn(Ph2L)]ClO_4	4.86		1000 (500), 600[f] (630), 450[f] (4100)
[Mn(Me3L)]$ClO_4 \cdot CH_2Cl_2$	4.87		880 (380), 600[f] (440)

[a] In the solid state at 298 K. [b] Solvent is dichloromethane. [c] Dichloromethane–toluene (1:1) at 300 K. [d] Polycrystalline state at 300 K. [e] Polycrystalline state at 77 K. [f] Shoulder.

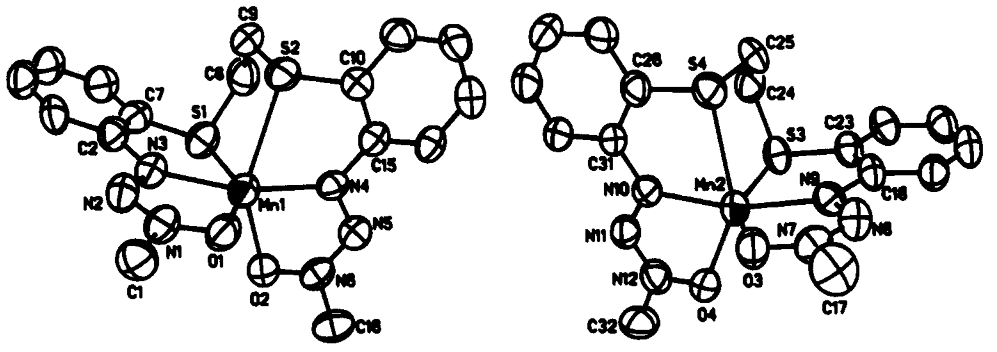

Figure 2. ORTEP plot and atom-labeling scheme for Mn(Me2L) with all atoms represented by their 50% probability ellipsoids.

abbreviated as H_2RxL (R = Me, Ph; *x* = 2, 3). The reaction of H_2RxL with manganese(II) acetate tetrahydrate in dichloromethane–methanol solution afforded pink bivalent complexes of composition Mn(R*x*L) in excellent yields. Constant-potential coulometric oxidation of Mn(R*x*L) in acetonitrile or dichloromethane afforded brown trivalent chelates isolated as [Mn(R*x*L)]Y where $Y^- = PF_6^-$, ClO_4^-. Selected characterization data for the complexes are given in Table I.

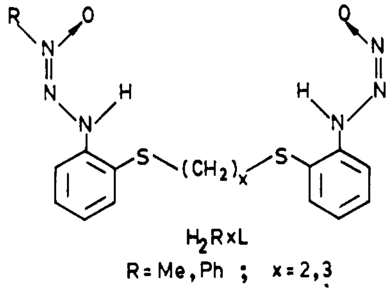

1

The [Mn(R*x*L)]Y species are 1:1 electrolytes with Λ = 130–150 $\Omega^{-1}\,cm^2\,M^{-1}$ in acetonitrile, and display a characteristic absorption band of moderate intensity near 1000 nm. Vibrations due to the N_3 and NO moieties of the triazene 1-oxide chelate rings[11] are observed in the ranges 1460–1485 and 1220–1230 cm^{-1}, respectively.

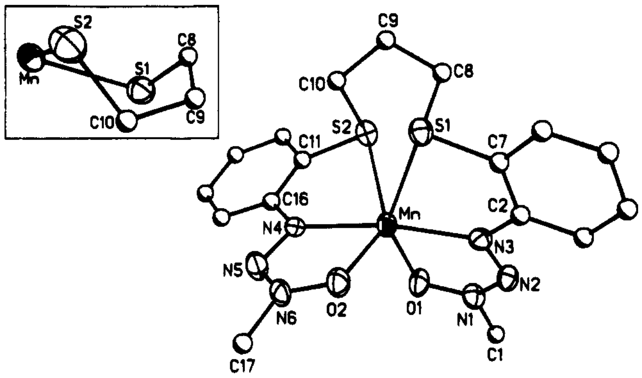

Figure 3. Perspective view and atom-labeling scheme for Mn(Me3L) with atoms other than carbon represented by their 50% probability ellipsoids. The configuration of the MnS_2C_3 chelate ring is shown in the inset.

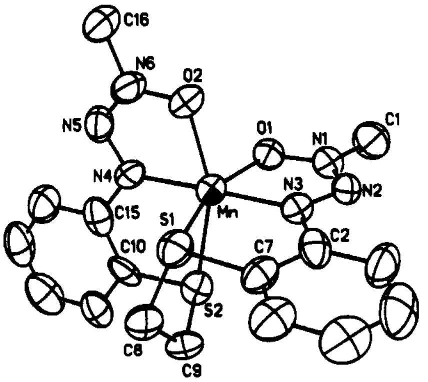

Figure 4. ORTEP plot and atom-labeling scheme for $[Mn(Me2L)]^+$ with all atoms represented by their 50% probability ellipsoids.

Both Mn(R*x*L) and $Mn(RxL)^+$ are high-spin with $S = {}^5/_2$ and 2, respectively. The former is EPR-active, but the latter is expectedly not so.[7c,12] The X-band EPR spectra of one representative complex, viz. Mn(Me2L), is shown in Figure 1. In the polycrystalline state (300 and 77K) and in fluid solution (300 K), the dominant feature is a broad signal with the *g* values in the region 2.009–5.135 (Table I). No ^{55}Mn hyperfine splitting is observed. In frozen glass (77 K), superior resolution is achieved and multiple features spread over a wide range become observable due to zero-field splitting in the distorted metal environments.[13,14] The presence of a strong signal (only this signal has signs of ^{55}Mn hyperfine structure) in the region 1350–1600 G suggests that the ligand field has an appreciable rhombic component.[14] The geometric distortions in Mn(R*x*L) have been quantitated in two cases through X-ray structure determinations.

Structure. The X-ray structures of Mn(Me2L), Mn(Me3L), and [Mn(Me2L)]$PF_6 \cdot CH_2Cl_2$ have been determined. In Mn(Me2L), two crystallographically distinct but metrically very similar molecules (Figure 2) constitute the asymmetric unit. The asymmetric unit of Mn(Me3L) has a single molecule (Figure 3). The structure of [Mn(Me2L)]$PF_6 \cdot CH_2Cl_2$ consists of discrete $[Mn(Me2L)]^+$ (Figure 4) and PF_6^- ions and CH_2Cl_2 molecules.

---

(11) Dutta, R. L.; Sharma, R. *J. Inorg. Nucl. Chem.* **1980**, *42*, 1204.

(12) Dexheimer, S. L.; Gohdes, J. W.; Chan, M. K.; Hagen, K. S.; Armstrong, W. H.; Klein, M. P. *J. Am. Chem. Soc.* **1989**, *111*, 8923.

(13) Basu, P.; Pal, S.; Chakravorty, A. *Inorg. Chem.* **1988**, *27*, 1850.

(14) (a) Wickman, H. H.; Klein, M. P.; Shirley, D. A. *J. Chem. Phys.* **1965**, *42*, 2113. (b) Dowsing, R. D.; Gibson, J. F. *J. Chem. Phys.* **1969**, *50*, 294. (c) Dowsing, R. D.; Gibson, J. F.; Goodgame, M.; Hayward, P. J. *J. Chem. Soc. A* **1969**, 187.

Table II. Selected Bond Distances (Å) and Angles (deg) and Their Estimated Standard Deviations for Mn(Me2L)

Distances			
Mn(1)-S(1)	2.677(3)	Mn(2)-S(3)	2.699(3)
Mn(1)-S(2)	2.730(3)	Mn(2)-S(4)	2.698(3)
Mn(1)-O(1)	2.146(6)	Mn(2)-O(3)	2.095(7)
Mn(1)-O(2)	2.105(6)	Mn(2)-O(4)	2.118(7)
Mn(1)-N(3)	2.141(6)	Mn(2)-N(9)	2.136(7)
Mn(1)-N(4)	2.142(6)	Mn(2)-N(10)	2.145(6)
O(1)-N(1)	1.315(7)	O(3)-N(7)	1.318(10)
O(2)-N(6)	1.318(8)	O(4)-N(12)	1.323(10)
N(1)-N(2)	1.279(11)	N(7)-N(8)	1.271(11)
N(2)-N(3)	1.336(10)	N(8)-N(9)	1.331(11)
N(4)-N(5)	1.334(9)	N(10)-N(11)	1.334(11)
N(5)-N(6)	1.294(12)	N(11)-N(12)	1.270(9)

Angles			
O(1)-Mn(1)-O(2)	95.2(2)	O(3)-Mn(2)-O(4)	98.0(3)
O(1)-Mn(1)-N(3)	72.1(3)	O(3)-Mn(2)-N(9)	72.6(3)
O(1)-Mn(1)-N(4)	119.2(3)	O(3)-Mn(2)-N(10)	122.2(2)
O(1)-Mn(1)-S(1)	146.3(2)	O(3)-Mn(2)-S(3)	147.0(2)
O(1)-Mn(1)-S(2)	104.8(2)	O(3)-Mn(2)-S(4)	98.5(2)
O(2)-Mn(1)-N(3)	119.1(3)	O(4)-Mn(2)-N(9)	118.2(2)
O(2)-Mn(1)-N(4)	72.7(2)	O(4)-Mn(2)-N(10)	72.9(2)
O(2)-Mn(1)-S(1)	96.2(2)	O(4)-Mn(2)-S(3)	98.3(2)
O(2)-Mn(1)-S(2)	146.0(2)	O(4)-Mn(2)-S(4)	147.7(2)
N(3)-Mn(1)-N(4)	164.3(3)	N(9)-Mn(2)-N(10)	161.6(3)
N(3)-Mn(1)-S(1)	74.6(2)	N(9)-Mn(2)-S(3)	74.4(2)
N(3)-Mn(1)-S(2)	93.5(2)	N(9)-Mn(2)-S(4)	93.2(2)
N(4)-Mn(1)-S(1)	94.5(2)	N(10)-Mn(2)-S(3)	89.9(2)
N(4)-Mn(1)-S(2)	73.6(2)	N(10)-Mn(2)-S(4)	74.8(2)
S(1)-Mn(1)-S(2)	82.3(1)	S(3)-Mn(2)-S(4)	82.3(1)

Table III. Selected Bond Distances (Å) and Angles (deg) and Their Estimated Standard Deviations for Mn(Me3L)

Distances			
Mn-S(1)	2.747(4)	O(1)-N(1)	1.317(12)
Mn-S(2)	2.783(4)	O(2)-N(6)	1.304(13)
Mn-O(1)	2.123(8)	N(1)-N(2)	1.254(13)
Mn-O(2)	2.118(7)	N(2)-N(3)	1.337(13)
Mn-N(3)	2.120(9)	N(4)-N(5)	1.329(13)
Mn-N(4)	2.137(9)	N(5)-N(6)	1.271(15)

Angles			
O(1)-Mn-O(2)	105.2(3)	O(2)-Mn-S(1)	94.7(2)
O(1)-Mn-N(3)	72.6(3)	O(2)-Mn-S(2)	139.8(2)
O(1)-Mn-N(4)	99.1(3)	N(3)-Mn-N(4)	169.7(4)
O(1)-Mn-S(1)	143.9(2)	N(3)-Mn-S(1)	73.6(2)
O(1)-Mn-S(2)	98.4(2)	N(3)-Mn-S(2)	114.1(3)
O(2)-Mn-N(3)	103.8(3)	N(4)-Mn-S(1)	115.7(3)
O(2)-Mn-N(4)	72.1(3)	N(4)-Mn-S(2)	72.5(2)
		S(1)-Mn-S(2)	84.2(1)

Table IV. Selected Bond Distances (Å) and Angles (deg) and Their Estimated Standard Deviations for [Mn(Me2L)]$PF_6 \cdot CH_2Cl_2$

Distances			
Mn-S(1)	2.502(4)	O(1)-N(1)	1.358(15)
Mn-S(2)	2.500(4)	O(2)-N(6)	1.329(15)
Mn-O(1)	2.047(8)	N(1)-N(2)	1.237(14)
Mn-O(2)	2.039(9)	N(2)-N(3)	1.339(15)
Mn-N(3)	1.946(9)	N(4)-N(5)	1.306(16)
Mn-N(4)	1.947(9)	N(5)-N(6)	1.252(15)

Angles			
O(1)-Mn-O(2)	93.6(3)	O(2)-Mn-S(2)	157.3(3)
O(1)-Mn-N(3)	76.9(4)	N(3)-Mn-N(4)	178.1(4)
O(1)-Mn-N(4)	103.3(4)	N(3)-Mn-S(1)	81.4(3)
O(1)-Mn-S(1)	158.4(3)	N(3)-Mn-S(2)	96.9(3)
O(1)-Mn-S(2)	94.9(2)	N(4)-Mn-S(1)	98.4(3)
O(2)-Mn-N(3)	105.5(4)	N(4)-Mn-S(2)	81.2(3)
O(2)-Mn-N(4)	76.3(4)	S(1)-Mn-S(2)	87.8(1)
O(2)-Mn-S(1)	92.0(3)		

Selected bond parameters of the complexes are listed in Tables II–IV. Some features common to the three complexes will be noted. The thioether functions are coordinated, and the ligands act in a hexadentate fashion, affording $MnS_2N_2O_2$ coordination spheres which display large angular distortions from octahedral symmetry due to constraints (such as acute chelate bite angles) inherent in multiple chelation. The five-membered rings incorporating N,O and N,S chelation constitute good to excellent planes. The trend in N–N lengths is consistent with the triazene 1-oxide formulation of the nitrogenous part of the ligand $-N(O)N{=}N^{-}-$. In both Mn(Me2L) and [Mn(Me2L)]$PF_6 \cdot CH_2Cl_2$, the dimethylene bridges have gauche configurations. In Mn(Me3L) the six-membered MnS_2C_3 chelate ring is a skew-boat (inset, Figure 3).

In Mn(Me2L) and Mn(Me3L), we have the first structural characterization of Mn^{II}–S(thioether) binding. The Mn–S lengths span the range 2.677(3)–2.783(4) Å, those in Mn(Me3L) lying on the higher side of the range. Structure determination[10,15] of a few other distorted octahedral 3d M^{II}(R*x*L) type species have afforded the following average M–S(thioether) lengths: Co–S, 2.53 Å; Ni–S, 2.51 Å; Zn–S, 2.68 Å (compare Mn–S = 2.72 Å). These lengths do not show any regular correlation with ionic radii (Mn^{2+}, 0.97 Å; Co^{2+}, 0.89 Å; Ni^{2+}, 0.83 Å; Zn^{2+}, 0.88 Å).[16] In d^5 Mn(R*x*L) as well as d^{10} Zn(R*x*L) the M–S lengths are too long, signifying the inherent weakness of metal–thioether affinity in these cases.

From Mn(Me2L) to [Mn(Me2L)]$PF_6 \cdot CH_2Cl_2$, the average Mn–S(thioether) length decreases by $\sim$0.2 Å, consistent with the decrease of metal radius upon oxidation. This is the first instance of comparison of Mn–S(thioether) lengths for the bivalent and trivalent metal in the same ligand environment. A consequence of the radial contraction upon metal oxidation is the significant increase in chelate bite angles (Table IV) in going from Mn(Me2L) to [Mn(Me2L)]$^+$. The cumulative effect for two contiguous chelate rings is reflected in the relatively large increase in the angles subtended at the metal atom by donor sites located in mutually trans positions: Mn(Me2L), 146.0(3)–164.3(3)°; [Mn(Me2L)]$^+$, 157.3(3)–178.1(4)° (Tables II and IV). High-spin manganese(III) is Jahn–Teller active in octahedral symmetry. However, even Mn(Me2L) and Mn(Me3L) display severe distortions due to the ligand constraints, and the observed distortions in [Mn(Me2L)]$^+$ are believed to be primarily due to the same reason.

To our knowledge the X-ray structures of only three complexes incorporating Mn–S(thioether) bonds have been reported so far. Two of these[4,5] are thioether-substituted carbonyl complexes of manganese(I) with relatively short Mn–S(thioether) lengths ($\sim$2.33 Å), consistent with the spin-paired d^6 configuration. The third example[6] is a high-spin manganese(III) salen type complex with relatively weak linkage to a pendant thioether function (Mn–S = 2.798(1) Å).

Electrochemical Interconversion. The transformation between Mn(R*x*L) and [Mn(R*x*L)]$^+$ is voltammetrically observable. Well-defined cyclic peaks at the same potentials are afforded by Mn(R*x*L) (initial scan anodic) and [Mn(R*x*L)]$^+$ (initial scan cathodic). The electrode process is quasireversible with peak-to-peak separations of 70–90 mV. The $E_{1/2}$ values for the [Mn(R*x*L)]$^+$–Mn(R*x*L) couples at 298 K are 0.37, 0.48, and 0.42 V vs SCE, respectively, for R = Me, $x = 2$; R = Ph, $x = 2$; and R = Me, $x = 3$. The Mn(Ph2L) complex is more difficult to oxidize than the Mn(Me2L) complex, as expected on the basis of substituent effects of the R groups. Coulometric oxidation of Mn(R*x*L) at 0.6 V affords [Mn(R*x*L)]$^+$ quantitatively via transfer of one electron, and this reaction was utilized for synthesis of [Mn(R*x*L)]Y. Reduction of [Mn(R*x*L)]$^+$ at 0.2 V leads to quantitative re-formation of Mn(R*x*L).

Concluding Remarks

The main findings and conclusions of this work will now be stated. The H_2R*x*L ligands have successfully afforded high-spin complexes of the types Mn^{II}(R*x*L) and [Mn^{III}(R*x*L)]Y incorporating Mn–S(thioether) bonds. The Mn(R*x*L)$^+$–Mn(R*x*L) reduction potential lies near 0.4 V vs SCE, and the two species are quantitatively electrointerconvertible.

---

(15) Chakraborty, P.; Chandra, S. K.; Chakravorty, A. Unpublished results.
(16) Shannon, R. D. *Acta Crystallogr.* **1976**, *A32*, 751.

Table V. Crystallographic Data for Mn(Me2L), Mn(Me3L), and [Mn(Me2L)]PF_6·CH_2Cl_2

	Mn(Me2L)	Mn(Me3L)	[Mn(Me2L)]PF_6·CH_2Cl_2
chem formula	$C_{16}H_{18}N_6O_2S_2Mn$	$C_{17}H_{20}N_6O_2S_2Mn$	$C_{17}H_{20}N_6O_2S_2Cl_2PF_6Mn$
fw	445.4	459.5	675.4
space group	*P*2₁/*a*	*P*2₁/*n*	*P*2₁/*n*
a, Å	19.465(6)	7.774(3)	12.361(3)
b, Å	7.933(4)	10.033(5)	14.621(3)
c, Å	26.644(7)	25.583(14)	14.941(3)
β, deg	110.19(2)	92.19(4)	101.24(2)
V, Å	3861(2)	1994(1)	2649(1)
Z	8	4	4
T, °C	23	23	23
λ, Å	0.710 73	0.710 73	0.710 73
ρ_{calcd}, g cm^{-3}	1.532	1.530	1.694
μ, cm^{-1}	8.88	8.98	9.62
transm coeff	0.6982–0.7523	0.6659–0.7234	0.6853–0.7725
R,[a] %	6.27	5.40	7.68
R_w,[b] %	6.59	5.50	6.70
GOF[c]	1.77	0.83	0.95

[a] $R = \sum||F_o| - |F_c||/\sum|F_o|$. [b] $R_w = [\sum w(|F_o| - |F_c|)^2/\sum w|F_o|^2]^{1/2}$; $w^{-1} = \sigma^2(|F_o|) + g|F_o|^2$; $g = 0.000\,01$ for Mn(Me2L), 0.000 04 for Mn(Me3L), and 0.000 01 for [Mn(Me2L)]PF_6·CH_2Cl_2. [c] The goodness of fit is defined as $[w(|F_o| - |F_c|)^2/(n_o - n_v)]^{1/2}$, where n_o and n_v denote the numbers of data and variables, respectively.

The first structural characterizations of Mn^{II}–S(thioether) bonds have been achieved in the form of Mn(Me2L) and Mn(Me3L): the range of the lengths is 2.677(3)–2.783(3) Å. In Mn(Me2L)$^+$, the average Mn–S(thioether) length is ~0.2 Å shorter than that in Mn(Me2L).

The $MnS_2N_2O_2$ family reported here augments the very meager list of authentic thioether-ligated manganese species known at present. Even though the Mn–S(thioether) link is inherently weak, especially when the metal is bivalent, judicious use of multidentate ligands bearing anionic charges can sustain it well. Further work on this theme is in progress.

Experimental Section

Materials. The purification of acetonitrile and dichloromethane and the preparation of tetraethylammonium perchlorate (TEAP) for electrochemical work were done as before.[7c] All other chemicals and solvents were of analytical grade and were used as obtained.

Physical Measurements. Electronic spectra were recorded with a Hitachi 330 spectrophotometer, and IR spectra were collected with a Perkin-Elmer Model 783IR spectrophotometer. Magnetic susceptibilities of solids were measured by using a PAR-155 vibrating-sample magnetometer fitted with a Walker Scientific L75FBAL magnet, and EPR spectra were recorded in the X-band using a Varian 109C spectrometer fitted with a quartz dewar. Calibration was done with DPPH (*g* = 2.0037). A Perkin-Elmer 240C elemental analyzer was used to collect microanalytical data (C, H, N). Electrochemical measurements were performed on a PAR Model 370-4 electrochemistry system as reported earlier.[7c] All potentials in this work are uncorrected for junction contribution. Solution (~10^{-3} M) electrical conductivities were measured with the help of a Philips PR 9500 bridge.

Preparation of Compounds. Ligands. The two amines 1,2-bis((2-aminophenyl)thio)ethane and 1,3-bis((2-aminophenyl)thio)propane were synthesized by following a reported method.[17] From these were also prepared the ligands H_2RxL by reported methods.[10,18,19]

Complexes. [1,2-Bis((*o*-(1-methyl-1-oxidotriazen-3-yl)phenyl)thio)ethanato-*N*^{3},*S*,*O*]manganese(II), Mn(Me2L). To a dichloromethane solution (15 mL) of H_2Me2L (0.20 g, 0.50 mmol) was added 0.060 g (~1 mmol) of KOH in methanol (10 mL), and the reaction mixture was stirred in air at room temperature for 0.5 h. A methanolic solution (10 mL) of $Mn(CH_3COO)_2\cdot 4H_2O$ (0.125 g, 0.50 mmol) was then added, and the reaction mixture was stirred for a further 2 h. A light-pink solid precipitated, was collected by filtration, and washed with methanol and water. The product was then dried in vacuo over P_4O_{10}. The yield was 0.186 g (~82%). Anal. Calcd for $C_{16}H_{18}N_6O_2S_2Mn$: C, 43.16; H, 4.04; N, 18.87; Mn, 12.34. Found: C, 43.12; H, 4.01; N, 18.83; Mn, 12.22.

Table VI. Atomic Coordinates (×10^4) and Equivalent Isotropic Displacement Coefficients (Å^2 × 10^3) for Mn(Me2L)[a]

atom	*x*	*y*	*z*	*U*(eq)
Mn(1)	3244(1)	4260(2)	3709(1)	55(1)
Mn(2)	−363(1)	2901(2)	1305(1)	51(1)
S(1)	2476(1)	5887(4)	4221(1)	65(1)
S(2)	3804(1)	7406(3)	3690(1)	58(1)
S(3)	273(1)	5971(3)	1442(1)	57(1)
S(4)	−1598(1)	4759(3)	951(1)	59(1)
O(1)	4135(3)	2576(8)	3780(2)	61(2)
O(2)	2418(3)	2524(8)	3311(2)	62(2)
O(3)	−756(3)	916(8)	1649(2)	64(2)
O(4)	454(3)	1546(8)	1117(2)	64(2)
N(1)	4528(4)	2232(10)	4280(3)	55(3)
N(2)	4411(4)	2846(10)	4687(2)	55(3)
N(3)	3844(4)	3909(10)	4543(3)	53(3)
N(4)	2640(3)	5313(9)	2943(3)	47(3)
N(5)	2126(4)	4365(11)	2597(3)	54(3)
N(6)	2047(3)	2951(11)	2813(3)	55(3)
N(7)	−682(4)	1157(10)	2154(3)	55(3)
N(8)	−385(3)	2466(11)	2415(2)	54(3)
N(9)	−159(4)	3545(10)	2123(3)	51(3)
N(10)	−613(4)	3111(9)	458(2)	50(3)
N(11)	−121(4)	2496(10)	262(2)	56(3)
N(12)	403(4)	1742(10)	612(3)	60(3)
C(1)	5107(5)	983(12)	4364(4)	64(4)
C(2)	3747(5)	4739(12)	4979(3)	56(4)
C(3)	4233(5)	4628(12)	5505(3)	59(4)
C(4)	4100(6)	5507(14)	5915(3)	69(4)
C(5)	3483(6)	6501(14)	5811(3)	71(4)
C(6)	3004(6)	6600(13)	5304(3)	67(4)
C(7)	3123(5)	5747(13)	4880(3)	58(4)
C(8)	2590(6)	8035(13)	4030(4)	73(4)
C(9)	3365(6)	8557(13)	4089(3)	76(5)
C(10)	3263(4)	7969(12)	3026(3)	48(3)
C(11)	3408(5)	9486(12)	2813(3)	58(4)
C(12)	3029(5)	9901(13)	2289(3)	60(4)
C(13)	2495(5)	8827(14)	1980(3)	64(4)
C(14)	2337(4)	7328(13)	2186(3)	54(3)
C(15)	2723(4)	6868(12)	2710(3)	48(3)
C(16)	1515(5)	1762(13)	2499(4)	72(4)
C(17)	−1000(6)	−85(14)	2407(4)	83(5)
C(18)	159(4)	5024(12)	2406(3)	50(3)
C(19)	298(5)	5227(13)	2953(3)	59(4)
C(20)	615(5)	6723(14)	3198(3)	69(4)
C(21)	799(5)	7971(14)	2915(3)	65(4)
C(22)	672(5)	7761(13)	2372(3)	59(4)
C(23)	360(4)	6283(12)	2119(3)	50(3)
C(24)	−512(5)	7246(13)	1075(3)	68(4)
C(25)	−1216(6)	6832(12)	1164(4)	70(4)
C(26)	−1708(5)	4752(12)	262(3)	53(3)
C(27)	−2316(5)	5536(13)	−97(4)	67(4)
C(28)	−2424(6)	5547(15)	−637(4)	82(5)
C(29)	−1913(6)	4776(14)	−813(3)	79(5)
C(30)	−1319(5)	3977(12)	−470(3)	65(4)
C(31)	−1193(4)	3938(11)	79(3)	49(3)
C(32)	999(5)	1000(15)	470(4)	80(5)

[a] Equivalent isotropic *U* is defined as one-third of the trace of the orthogonalized U_{ij} tensor.

The complexes Mn(Ph2L) and Mn(Me3L) were similarly prepared (yield ~75%). Anal. Calcd for $C_{26}H_{22}N_6O_2S_2Mn$ (Mn(Ph2L)): C, 54.85; H, 3.86; N, 14.75; Mn, 9.65. Found: C, 54.82; H, 3.84; N, 14.62; Mn, 9.48. Anal. Calcd for $C_{17}H_{20}N_6O_2S_2Mn$ (Mn(Me3L)): C, 44.47; H, 4.35; N, 18.29; Mn, 11.97. Found: C, 44.18; H, 4.27; N, 18.10; Mn, 11.68.

[1,2-Bis((*o*-(1-methyl-1-oxidotriazen-3-yl)phenyl)thio)ethanato-*N*^{3},*S*,*O*]manganese(III) Hexafluorophosphate, [Mn(Me2L)]PF_6·CH_2Cl_2. A 20-mL solution of Mn(Me2L) (0.04 g, 0.09 mmol) in acetonitrile containing 0.40 g of NH_4PF_6 (supporting electrolyte) was subjected to constant-potential coulometric oxidation at 0.60 V vs SCE. The oxidation was complete at a count 8.49 C (the calculated count for one-electron transfer was 8.67 C). The color of the solution changed from light-pink to deep brown. The solution was then evaporated to dryness in vacuo, and the solid was extracted with dichloromethane. The extract was filtered, the filtrate was layered with *n*-hexane in 1:3 ratio, and the mixture was kept

---

(17) Unger, O. *Chem. Ber.* **1897**, *30*, 607.
(18) Zacharias, P. S.; Chakravorty, A. *Inorg. Chem.* **1971**, *10*, 1961.
(19) Mukkanti, K.; Bhoon, Y. K.; Pandeya, K. B.; Singh, R. P. *J. Indian Chem. Soc.* **1982**, *59*, 830.

Table VII. Atomic Coordinates ($\times 10^4$) and Equivalent Isotropic Displacement Coefficients ($Å^2 \times 10^3$) for Mn(Me3L)[a]

atom	*x*	*y*	*z*	*U*(eq)
Mn	50(2)	2287(2)	1246(1)	42(1)
S(1)	–991(4)	4832(3)	1472(1)	46(1)
S(2)	–3449(4)	1822(3)	1058(1)	50(1)
O(1)	1008(11)	1051(7)	650(3)	55(3)
O(2)	1930(10)	2199(8)	1866(3)	59(3)
N(1)	1793(13)	1735(10)	289(3)	49(4)
N(2)	1941(12)	2979(9)	287(3)	45(4)
N(3)	1171(12)	3551(8)	689(3)	42(4)
N(4)	–711(11)	776(9)	1779(3)	40(3)
N(5)	409(15)	406(10)	2156(3)	56(4)
N(6)	1698(13)	1185(11)	2175(3)	53(4)
C(1)	2555(17)	957(12)	–129(5)	62(3)
C(2)	1328(16)	4920(12)	687(4)	44(4)
C(3)	2387(17)	5651(12)	352(4)	54(5)
C(4)	2441(20)	7000(13)	359(5)	69(6)
C(5)	1435(18)	7710(13)	697(5)	64(5)
C(6)	457(17)	7036(11)	1040(4)	54(5)
C(7)	358(15)	5649(11)	1033(4)	39(4)
C(8)	–3003(15)	4949(12)	1094(4)	53(3)
C(9)	–4465(17)	4313(12)	1391(5)	65(4)
C(10)	–4150(16)	2904(12)	1582(4)	57(3)
C(11)	–3489(16)	287(11)	1400(4)	48(3)
C(12)	–4967(17)	–508(12)	1343(4)	59(3)
C(13)	–5024(20)	–1693(14)	1625(5)	80(4)
C(14)	–3709(17)	–2048(14)	1963(5)	67(4)
C(15)	–2288(16)	–1247(12)	2026(4)	54(3)
C(16)	–2154(15)	–60(11)	1748(4)	45(3)
C(17)	3074(17)	893(13)	2556(5)	72(4)

[a] Equivalent isotropic *U* is defined as one-third of the trace of the orthogonalized U_{ij} tensor.

in a refrigerator, yielding dark crystals in 4–5 days (yield 0.041 g, 78%). Anal. Calcd for $C_{17}H_{20}N_6O_2S_2Cl_2PF_6Mn$: C, 30.24; H, 2.96; N, 12.44; Mn, 8.14. Found: C, 30.20; H, 2.88; N, 12.18; Mn, 8.02.

The complexes [Mn(Ph2L)]ClO_4 and [Mn(Me3L)]ClO_4·CH_2Cl_2 were similarly synthesized respectively using acetonitrile and dichloromethane as the solvents for electrolysis with [Et_4N]ClO_4 as the supporting electrolyte. The dichloromethane extract of the residue obtained by evaporation of the electrolyzed solution was mixed with two volumes of *n*-hexane, and the solution was kept in the refrigerator. The crystalline complexes were collected by filtration and dried in vacuo over P_4O_{10} (yield ~70%). Anal. Calcd for $C_{26}H_{22}N_6O_6S_2ClMn$ ([Mn(Ph2L)]ClO_4): C, 46.69; H, 3.29; N, 12.56; Mn, 8.21. Found: C, 46.58; H, 3.34; N, 12.53; Mn, 8.16. Anal. Calcd for $C_{18}H_{22}N_6O_6S_2Cl_3Mn$ ([Mn(Me3L)]ClO_4·CH_2Cl_2): C, 33.58; H, 3.42; N, 13.06; Mn, 8.54. Found: C, 33.21; H, 3.51; N, 13.11; Mn, 8.52.

X-ray Structure Determination. Unless otherwise indicated the same description applies to all the three complexes. Cell parameters of Mn(Me2L) (0.18 × 0.26 × 0.44 mm^3), Mn(Me3L) (0.16 × 0.20 × 0.32 mm^3), and [Mn(Me2L)]PF_6·CH_2Cl_2 (0.12 × 0.20 × 0.42 mm^3) grown (298 K) by slow diffusion of hexane into dichloromethane solutions were determined by least-squares fits of 30 machine-centered reflections (2θ = 15–30°). Lattice dimensions and Laue groups were checked by axial photography. Systematic absences led to space group identification: $P2_1/n$ for Mn(Me3L) and [Mn(Me2L)]PF_6·CH_2Cl_2 and $P2_1/a$ for Mn(Me2L). Data were collected by the ω-scan method (2θ = 2–50°) on a Nicolet R3m/V diffractometer with graphite-monochromated Mo Kα (λ = 0.710 73 Å) radiation. Two check reflections measured after every 98 reflections showed no significant intensity reduction during ~70-h (Mn(Me2L)), ~36-h (Mn(Me3L)), and ~40-h ([Mn(Me2L)]PF_6·CH_2Cl_2) exposure to X-rays. Data were corrected for Lorentz–polarization effects and absorption.[20] Of the 7604 (Mn(Me2L)), 4305 (Mn(Me3L)), and 5119 ([Mn(Me2L)]PF_6·CH_2Cl_2) reflections collected, 6790 (Mn(Me2L)), 3524 (Mn(Me3L)), and 4643 ([Mn(Me2L)]PF_6·CH_2Cl_2) were unique, of which 3385 (Mn(Me2L)) and 1247 (Mn(Me3L)) satisfying $I > 3\sigma(I)$ and 1751 ([Mn(Me2L)]PF_6·CH_2Cl_2) satisfying $I > 2.5\sigma(I)$ were used for structure solutions.

Table VIII. Atomic Coordinates ($\times 10^4$) and Equivalent Isotropic Displacement Coefficients ($Å^2 \times 10^3$) for [Mn(Me2L)]PF_6·CH_2Cl_2[a]

atom	*x*	*y*	*z*	*U*(eq)
Mn	1846(2)	3574(1)	11974(1)	47(1)
Cl(1)	588(5)	292(3)	8884(3)	117(2)
Cl(2)	1646(6)	–365(5)	7491(4)	170(3)
S(1)	1212(3)	2502(2)	10675(2)	52(1)
S(2)	2192(3)	2204(2)	12996(2)	50(1)
O(1)	1738(7)	4472(5)	13001(6)	58(3)
O(2)	2194(7)	4573(6)	11118(6)	66(3)
N(1)	660(9)	4597(7)	13042(7)	53(4)
N(2)	–99(9)	4205(7)	12522(7)	48(4)
N(3)	265(7)	3655(7)	11929(6)	47(3)
N(4)	3430(7)	3457(7)	12043(7)	51(4)
N(5)	3919(8)	3987(8)	11541(8)	56(4)
N(6)	3260(10)	4542(7)	11084(7)	61(4)
P	9234(3)	2551(3)	14446(2)	57(1)
F(1)	8464(10)	3131(11)	13798(11)	210(8)
F(2)	9826(11)	2300(9)	13646(8)	162(7)
F(3)	10039(8)	1861(7)	15045(8)	127(5)
F(4)	8718(11)	2766(7)	15276(7)	154(7)
F(5)	10071(10)	3340(8)	14642(9)	151(6)
F(6)	8392(8)	1721(8)	14271(8)	139(5)
C(1)	408(12)	5228(9)	13722(9)	80(6)
C(2)	–558(10)	3119(9)	11372(8)	50(5)
C(3)	–1665(11)	3172(11)	11424(10)	70(6)
C(4)	–2405(12)	2613(12)	10855(11)	85(7)
C(5)	–2076(12)	2017(11)	10234(9)	71(6)
C(6)	–954(11)	1991(10)	10187(8)	64(5)
C(7)	–203(9)	2512(9)	10757(8)	49(4)
C(8)	1692(9)	1448(8)	11237(7)	56(4)
C(9)	1543(9)	1328(8)	12218(7)	49(4)
C(10)	3597(10)	2104(8)	12969(9)	52(5)
C(11)	4239(11)	1419(10)	13466(9)	61(5)
C(12)	5353(13)	1386(12)	13456(10)	80(6)
C(13)	5817(12)	1998(13)	12977(12)	82(7)
C(14)	5209(12)	2691(10)	12499(10)	73(6)
C(15)	4093(10)	2750(9)	12500(8)	56(5)
C(16)	3641(12)	5204(9)	10484(9)	79(6)
C(17)	1796(16)	181(13)	8512(14)	173(11)

[a] Equivalent isotropic *U* is defined as one-third of the trace of the orthogonalized U_{ij} tensor.

The structures were solved by direct methods. All non-hydrogen atoms of Mn(Me2L) and [Mn(Me2L)]PF_6·CH_2Cl_2 were made anisotropic. Due to paucity of observed data, only the following atoms were made anisotropic for Mn(Me3L): Mn, all O, all N, all S, and C(2)–C(7). Hydrogen atoms were added at calculated positions with fixed U = 0.08 $Å^2$ in the last cycle of refinement. All refinements were performed by full-matrix least-squares procedures. The highest residuals were 0.52 e/$Å^3$ (Mn(Me2L)), 0.40 e/$Å^3$ (Mn(Me3L)), and 0.67 e/$Å^3$ ([Mn(Me2L)]PF_6·CH_2Cl_2). All calculations were done on a MicroVAX II computer with the programs of SHELXTL-PLUS.[21] Significant crystal data are listed in Table V. Atomic coordinates and isotropic thermal parameters are collected in Tables VI (Mn(Me2L)), VII (Mn(Me3L)), and VIII ([Mn(Me2L)]PF_6·CH_2Cl_2).

Acknowledgment. Crystallography was performed at the National Single Crystal Diffractometer Facility, Department of Inorganic Chemistry, Indian Association for the Cultivation of Science. We are grateful to the Department of Science and Technology, New Delhi, for financial support. The Council of Scientific and Industrial Research provided a fellowship to P.C. Affiliation with the Jawaharlal Nehru Centre for Advanced Scientific Research, Bangalore, India, is acknowledged.

Supplementary Material Available: For Mn(Me2L), Mn(Me3L), and [Mn(Me2L)]PF_6·CH_2Cl_2, tables of complete bond distances (Tables S1, S5, and S9) and angles (Tables S2, S6, and S10), anisotropic thermal parameters (Tables S3, S7, and S11), and hydrogen atom positional parameters (S4, S8, and S12) (14 pages). Ordering information is given on any current masthead page.

---

(20) North, A. C. T.; Phillips, D. C.; Mathews, F. S. *Acta Crystallogr.* **1968**, *A24*, 351.

(21) Sheldrick, G. M. SHELXTL-PLUS 88. *Structure Determination Software Programs*; Nicolet Instrument Corp.: 5225-2 Verona Rd., Madison, WI 53711, 1988.